RSC Advances

ROYAL SOCIETY OF CHEMISTRY

www.rsc.org/advances

Optimizing Supercapacitor Electrode Density: Achieving the Energy of Organic Electrolytes with the Power of Aqueous Electrolytes.

M. D. Merrill, E. Montalvo, P. G. Campbell, Y. M. Wang, M. Stadermann, T. F. Baumann, J. Biener, M. A. Worsley*

Lawrence Livermore National Laboratory, Physical and Life Sciences Directorate, Livermore, California, United States.

*worsley1@llnl.gov

Abstract

The value of electrode density is often overlooked in the pursuit of impressive supercapacitor metrics. Low-density electrodes deliver the best performance in terms of gravimetric energy and power densities when only the mass of the electrodes is considered. However, energy and power values with respect to the total system mass (electrode + electrolyte) or volume are more meaningful for practical application. Low-density electrodes are impractical due to both large mass contributions by the electrolyte and large system volumes. Here, we use highly compressible graphene aerogel electrodes (up to 87.5% volumetric compression) to systematically characterize the effects of electrode density on energy and power metrics. The results reveal that electrode density is similar to electrode thickness in that both parameters have a squared effect on power. Accounting for the aqueous electrolyte's mass lowered the gravimetric energy and power by almost an order of magnitude for 0.144 g/cm^3 dense carbon electrodes but only by a factor of 1.5 when the electrode density was increased to 1.15 g/cm^3 through compression. The high-density electrodes achieve 8 Wh/kg, 70,000 W/kg, and 144 F/cm^3 in a symmetric electrode setup after factoring in the aqueous electrolyte's mass. Therefore, in the pursuit of high energy per mass, it can be just as effective to lower the system's mass with smaller electrolyte fractions as it is to use electrolytes with larger voltage ranges. High electrode densities allow aqueous electrolyte supercapacitors to attain energy densities per the system mass comparable to those of commercially-available organic electrolyte supercapacitors while maintaining 10 - 100× greater power.

Introduction

The best supercapacitor performance metrics are typically achieved with low-density carbon electrodes. The energy metric of F/g electrode mass is strongly dependent upon surface area and it is relatively easy to achieve high surface areas per electrode mass (>1,000 m^2/g) with low electrode densities [1-4]. Similarly, it is easy to achieve higher power in low-density electrodes because large, non-tortuous pores and diluted solution resistances per volume facilitate fast conduction of electrolyte ions [5-8]. The problem is that both the system's total volume and the mass of the electrolyte required to use these electrodes are typically neglected in the literature. Performance metrics of low-density electrodes are artificially enhanced with respect to higher density electrodes when the supercapacitor's volume and the electrolyte's mass are ignored. The energy or power per system mass (electrode + electrolyte) or volume are more important values in practical application than metrics only based upon the mass of the

electrode [9-11]. The effects of the electrolyte's mass on energy density are illustrated in Figure 1a, which indicates that graphitic supercapacitor electrodes with densities < 0.6 g/cm^3 show a significant decrease in energy density. Consequently, the value of high density electrodes has been recently noted by several groups [12-17] yet the effects of electrode density on energy and power have not been clearly characterized. Here, we systematically studied the dependence of energy and power per mass and volume on electrode density in the absence of other experimental artifacts by taking advantage of the graphene electrode's compressibility. By considering supercapacitor performances with respect to the total system's mass or volume (excluding packaging), the value of electrode density for practical performance metrics can be clearly observed.

Controlling the electrode density is ideally achieved without changing other influential parameters, such as surface area per electrode mass, ionic mass transport effects, or the distribution of the smallest pore sizes. A constant m^2/g with respect to density ideally results in a condition where the energy per total mass only changes due to the mass fraction of electrolyte. It has been reported that electrolytic double layer capacitance (EDLC) can be affected when pore sizes are comparable to those of the solvated ions and so it is also preferable to keep the smallest pore size distribution constant with respect to electrode density [18-20]. It is extremely difficult to deterministically control the electrode density through the materials synthesis methodology without affecting the other properties. Instead, in this report electrode density is controlled through the mechanical compression of monolithic graphene macro-assembly (GMA) electrodes after synthesis. The GMA electrodes are composed of well-exfoliated graphene sheets chemically cross-linked via strong, conductive sp^2 carbons bonds. These properties result in electrodes with high electrical conductivity, large surface areas, and excellent mechanical properties that allow high compression strains. [1]

The electrolyte's density is also a fundamentally important but rarely discussed value. Acetonitrile solvent electrolytes may have densities as low as 1.0 g/cm^3 while propylene carbonate solvent electrolytes reach 1.5 g/cm^3. Aqueous supercapacitor electrolytes of concentrated KOH or H_2SO_4 have densities around 1.3 – 1.4 g/cm^3. Both aqueous electrolytes facilitate high power densities because of their high conductivities. For example, a 26 wt.% KOH solution (6 M) reaches 625 mS/cm at 25 °C [21]. The drawback for these electrolytes is their limited voltage range of about 1 – 1.2 V, which severely limits the supercapacitor's gravimetric energy. Recent literature indicates that the stable voltage can reach up to 2 V in neutral pH, aqueous electrolytes [22-24]. Neutral electrolytes have much lower conductivities than concentrated KOH and H_2SO_4 electrolytes but this disadvantage can be offset by conductance. Conductance is dependent upon the voltage bias and so a 600 mS/cm electrolyte under a 1 V bias has the same conductance as a 300 mS/cm electrolyte under a 2 V bias. A good, neutral electrolyte would be 6 M CsCl because it has a conductivity of 340 mS/cm except that it would have a density of 2 g/cm^3. Factoring in the mass of an electrolyte with a 2 g/cm^3 density causes a large dilution in energy or power per mass metrics (Figure 1a). A better electrolyte is a 6 M LiCl electrolyte, whose conductivity has been enhanced by the viscosity-decreasing effects of an additional 1 M of CsCl because of how a high conductivity (180 mS/cm) can be combined with a relatively low electrolyte mass fraction (30 wt.% or 1.42 g/cm^3) [25]. The LiCl + CsCl electrolyte is also advantageous in that it is less corrosive than aqueous KOH electrolytes and less toxic than organic electrolytes.

Results and Discussion

The microstructure of the GMA allows uniaxial mechanical compression to change electrode thickness. TEM images indicate a sheet-like architecture with pore sizes below 100 nm (Figure 1b) confirming the mesoporous nature of the 3D graphene. The GMA has a high BET surface area of 1266 m^2/g, indicating that the graphene sheets in the GMA are, on average, two atomic layers thick. BJH (mesopore) and DFT (micropore) analysis (Figure 1c-d), reveals that the bulk of the surface area (1150 m^2/g) is due to sub-10-nm pores with a peak at 5 nm. This architecture indicates that 91 % of the surface area exists in < 10 nm pores while the remaining 9 % of the surface area belongs to the macropore (>50 nm) regime. It will be shown that insignificant changes in capacitance per electrode mass occurred upon compression to decrease electrode thickness by a factor of 8 and to increase electrode density from 0.144 g/cm^3 to 1.152 g/cm^3. This indicates that only the macropore structure collapses upon compressing the electrode and that negligible surface area is lost upon changing the electrode's density. (Figures S1, S2)

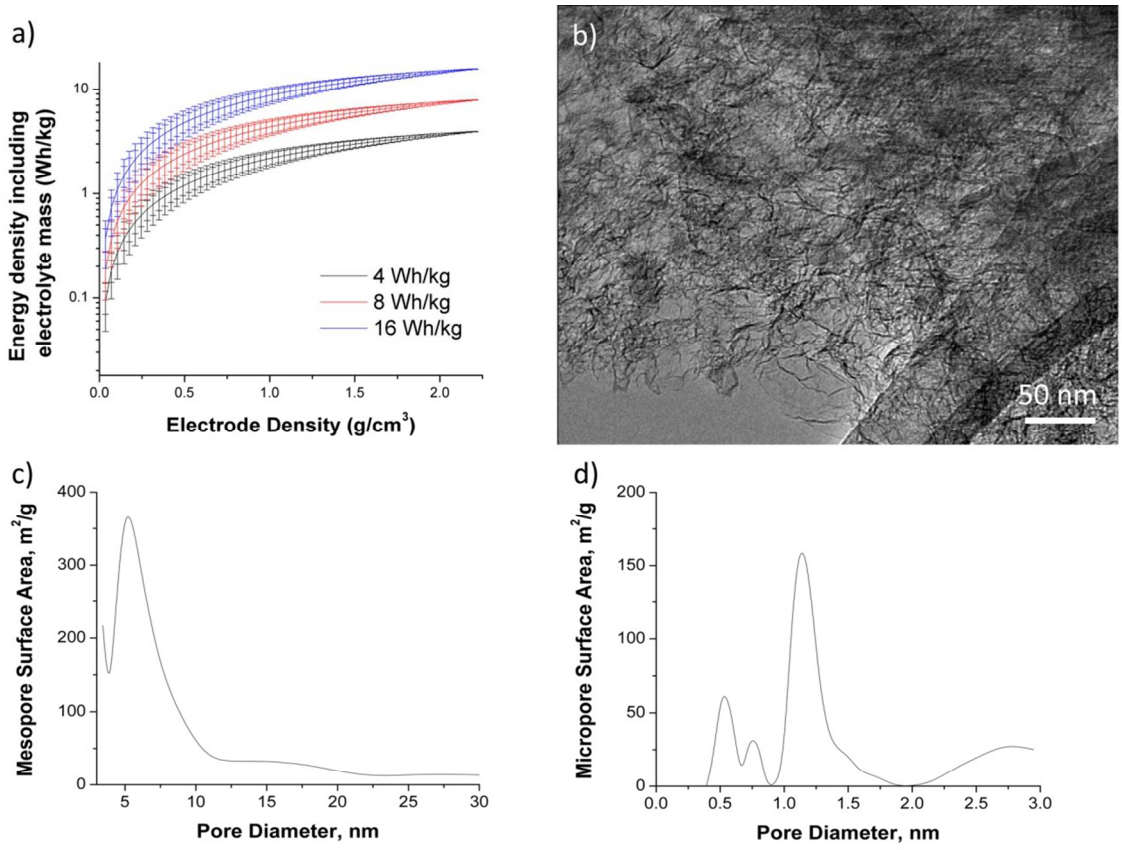

Figure 1. a) Electrolyte mass contribution. A practical consideration of gravimetric energy or power metrics includes both electrode and electrolyte masses. Graph for converting energy density determined using only electrode mass (4,8, and 16 Wh/kg) to energy density including electrode and electrolyte mass (y-axis) as a function of electrode density (x-axis). Density of electrolyte used in the plot is 1.5

g/cm^3. Error bars allow for +/- 0.5 g/cm^3.in electrolyte density b) TEM image of the GMA. Pore size distributions showing surface area in the c) mesopore and d) micropore regimes.

The GMA electrodes are capable of ultra-fast (dis)charge rates. The symmetric cell with uncompressed electrode densities (0.14 g/cm^3) and 125 µm thickness did not exhibit ohmic drop effects ≤ 60 A/g of electrode mass with the 5 M KOH electrolyte (Figure 2a). 1,000 µm thick electrodes compressed to a final density of 1.15 g/cm^3 and 125 µm thickness exhibited dramatically larger impedances as ohmic drop effects were only absent for ≤ 1 A/g electrode mass with the 5 M KOH electrolyte (Figure 2b). The factor of about 64 difference in the (dis)charge rates at which ohmic drop began affecting capacitance indicates the factor of 8 change in electrode density had an inverse squared effect on internal impedance. This inverse squared relationship between the (dis)charge rates at which ohmic drop begins affecting capacitance and the electrode density was observed for all compressed electrodes.

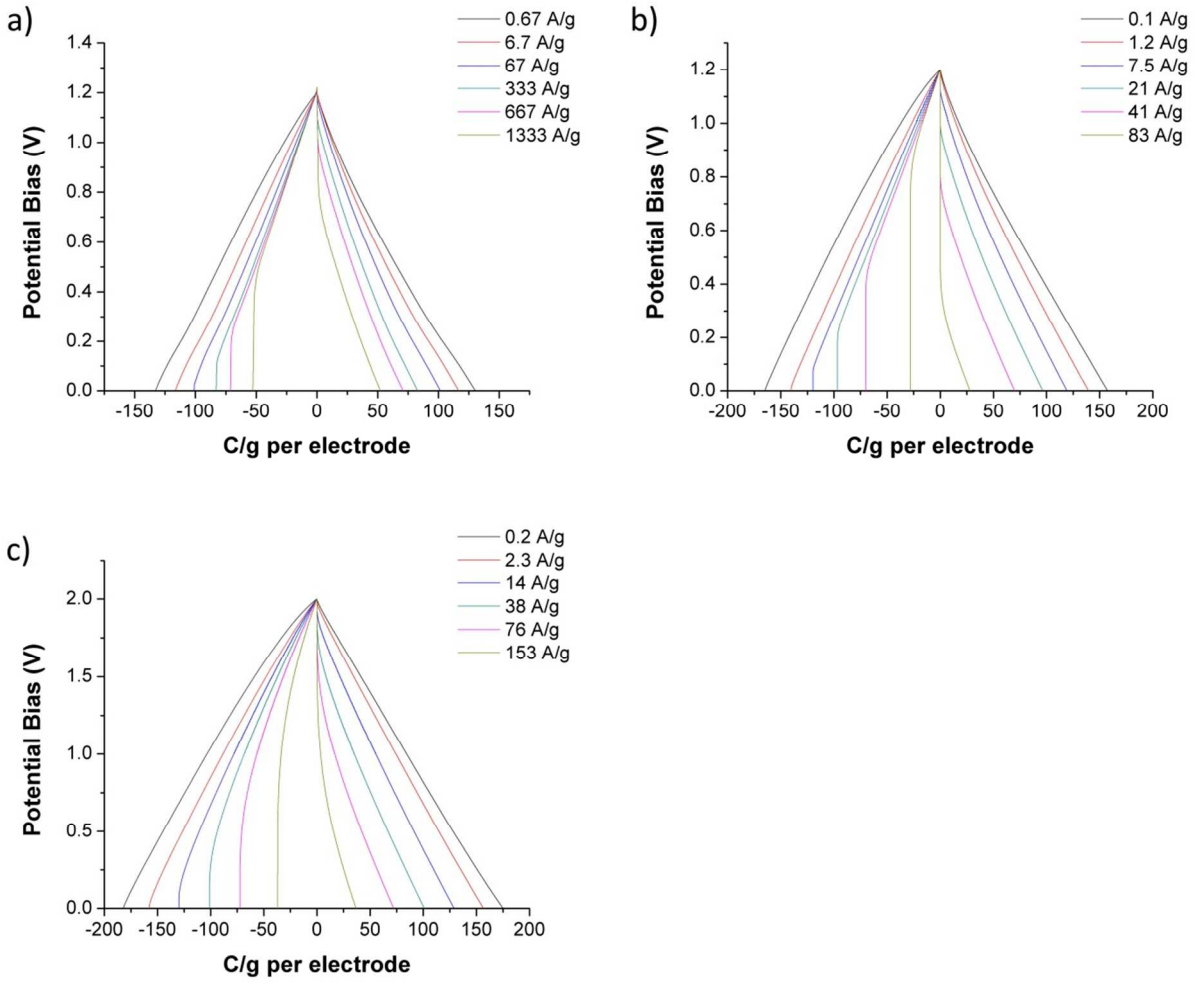

Figure 2. Galvanostatic (dis)charge curves in the symmetric, two-electrode setup. A) 125 µm thick GMA electrodes at 0.14 g/cm^3 density in 5 M KOH. B) 125 µm thick GMA electrodes compressed to 1.15 g/cm^3

density in 5 M KOH. C) 125 µm thick GMA electrodes compressed to 1.15 g/cm^3 density in 6 M LiCl + 1 M CsCl.

The neutral pH electrolytes were stable over a larger voltage range than the alkaline electrolyte. The 5 M KOH electrolyte was limited to only a voltage bias of 1.2 V while the 6 M LiCl + 1 M CsCl electrolyte could be charged up to 2.0 V (Figure 2c). The 1.15 g/cm^3 dense and 125 µm thick electrodes did not exhibit ohmic drop effects ≤ 2 A/g of electrode mass. Impedance caused by ohmic drop initiated at slower (dis)charge rates for the 5 M KOH electrolyte (1 A/g electrode mass) than for the 6 M LiCl + 1 M CsCl electrolyte (2 A/g of electrode mass) at the same electrode density and thickness even though the 5 M KOH electrolyte's conductivity is about 3.5 times greater. The larger voltage range of the 6 M LiCl + 1 M CsCl electrolyte may compensate against solution resistance effects through conductance.

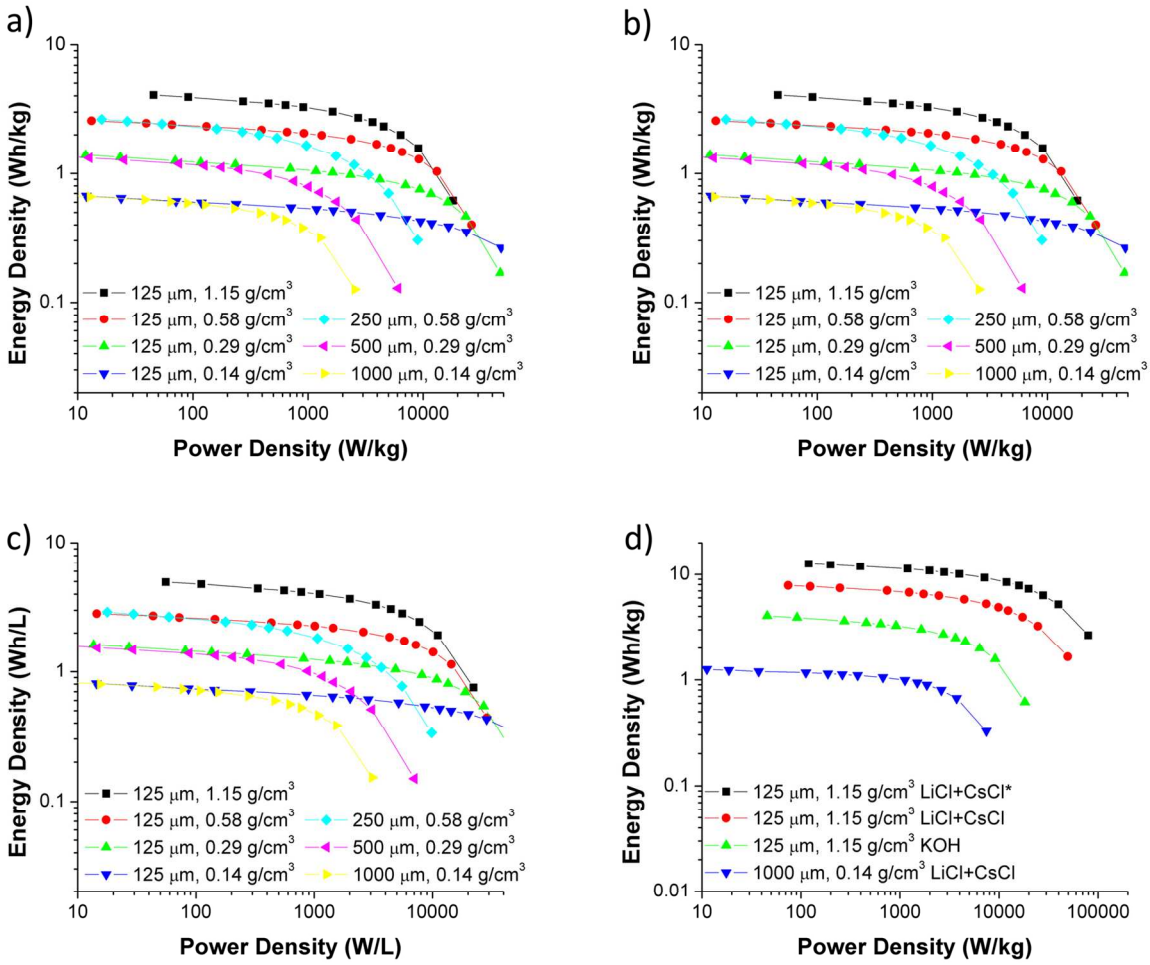

Figure 3. Ragone plots for symmetric, two electrode setups. A) Gravimetric energy and power per electrode mass with respect to GMA electrode thickness and density in 5 M KOH electrolyte. B) Gravimetric energy and power per system (electrode + electrolyte) mass with respect to GMA electrode thickness and compression in 5 M KOH electrolyte. C) Volumetric energy and power per system

(electrode + electrolyte) mass with respect to GMA electrode thickness and compression in 5 M KOH electrolyte. D) Gravimetric energy and power comparison for the GMA electrodes in aqueous KOH and 6 M LiCl + 1 M CsCl electrolytes (values are per system mass unless noted with *).

Electrode density and thickness had the same effects on energy and power per electrode mass (Figure 3a). The energy per electrode mass did not change with respect to the electrode's density or thickness for the slowest (dis)charge rates because all of the electrodes exhibited the same F/g of electrode mass. An insignificant change in F/g of electrode mass with electrode density indicates that mechanically compressing the electrodes did not significantly change surface area per mass. The electrode's thickness had a squared effect on power per electrode mass as expected. Interestingly, the power did not change upon compression of the electrode. The power density per electrode mass was therefore constant for a given electrode mass per footprint area in a given electrolyte. For example, the Ragone curve obtained for the 1,000 µm thick electrodes at 0.14 g/cm^3 density did not change when the electrodes were compressed to 125 µm and 1.15 g/cm^3. These results indicate that both electrode density and thickness limit power per electrode mass through an inverse square relationship and that higher density and thicker electrodes are inherently slower.

The electrode density has a dramatic effect on energy and power densities when the electrolyte mass fraction is also considered. The effects of electrode density are different from the effects electrode thickness when the electrolyte's mass contribution is also considered because electrode density affects the electrolyte mass fraction while electrode thickness does not. Accounting for the 5 M KOH electrolyte's mass dilutes the gravimetric energy density by a factor of 9 for the 0.14 g/cm^3 dense electrode because 94 % of the electrode's volume is occupied by electrolyte (Figure 3b). The 6.6 Wh/kg of electrode mass for the 0.14 g/cm^3 dense electrode does not appear to be practical when reported as a 0.7 Wh/kg system (electrode + electrolyte) energy density. The energy density of the 1.15 g/cm^3 dense electrode is only diluted by a factor of 1.5 to a 4 Wh/kg system energy density when the electrolyte's mass is considered. The changes in energy density, which occur when the electrolyte's mass is factored into the system's mass, also affects the power density because power density is a function of energy density according to equation (3). This means the power losses observed for the higher density electrodes in Figure 3a are partially offset by the contribution of the electrolyte's mass to energy density in Figure 3b. The effects of electrode density and thickness on volumetric energy and power (Figure 3c) are functionally the same as for gravimetric energy and power densities when the electrolyte's mass is considered (Figure 3b). Consideration of the electrolyte mass causes the highest density (125 µm, 1.15 g/cm^3) electrodes to have the best combinations of energy and power in Figures 3b-c even though it had worst combination of energy and power in Figure 3a. Consideration of only the electrode mass therefore dramatically misrepresents the practical performance metrics of the systems.

The 6 M LiCl + 1 M CsCl electrolyte outperformed the 5 M KOH electrolyte in energy and power but not in capacitance (F/g) per electrode mass). The LiCl + CsCl electrolyte achieves energies of up to 13 Wh/kg and powers up to 100,000 W/kg when only considering the electrode's mass (Figure 3d). Similar to the KOH electrolyte, the energy and power with respect to the electrodes mass for the LiCl + CsCl electrolyte did not change upon compressing the 1,000 µm, 0.144 g/cm^3 electrode to 125 µm, 1.15 g/cm^3. The LiCl + CsCl electrolyte exhibits over 8 Wh/kg and 70,000 W/kg for the 125 µm, 1.15 g/cm^3 system even after

factoring in the electrolyte's mass (Figure 3d). Both the energy and power densities of the LiCl + CsCl electrolyte are a factor of 2 greater than the values exhibited by the KOH electrolyte. The supercapacitor's energy, E, is a function of capacitance, C, and voltage range, V, according to equation (2).The capacitance per electrode mass of the GMA in the LiCl + CsCl electrolyte (C_{tot} = 23 F/g, C_{ind} = 93 F/g) is smaller than in the KOH electrolyte (C_{tot} = 33 F/g, C_{ind} = 132 F/g). The volumetric capacitance (C_{ind} = 144 F/cm^3) for the 1.15 g/cm^3 dense GMA electrodes in KOH electrolyte surpasses the practical minimum limit of 100 F/cm^3 [9-11]. The stable voltage range of the LiCl + CsCl system (2 V, Figure 2c) is much larger than that of the KOH electrolyte (1.2 V, Figure 2a) and the voltage range has an exponential effect on energy and according to equations (2) and (3).

Conclusions

In summary, we have shown that the electrode's density is a critical parameter for supercapacitor electrodes and the GMA electrodes are an excellent platform for considering the effects of electrode density on system energy and power because the electrode density could be directly tuned through mechanical compression. As such, the effects of electrode density and electrolyte mass were characterized without extraneous complications, such as significant changes in surface area per mass. The ideal behavior of the GMA electrodes was evident in that there was no significant change in energy or power per electrode mass with up to the factor of 8 increases in electrode density through mechanical compression. The main conclusions of this study are as follows:

1) The electrode densities need to be high (> 0.8 g/cm^3) so that the aqueous electrolyte mass fraction does not dilute energy and power by a factor greater than 2.
2) Both electrode density and thickness had an inverse squared effect on power density when only the electrode mass was considered.
3) Aqueous electrolyte supercapacitors (e.g. LiCl+CsCl) can compete with the system energy density (4-10 Wh/kg) of commercially available organic electrolyte supercapacitors if the electrode density is sufficiently high at 10-100x the power density.

This last point illustrates the fact that when considering energy per mass for supercapacitors, it can be just as effective to lower the system's mass with smaller electrolyte fractions as it is to use electrolytes with larger voltage ranges. The aqueous LiCl + CsCl electrolyte is also promising in that it is less corrosive than aqueous KOH and less toxic than the organic electrolytes.

Acknowledgements

This work was performed under the auspices of the U.S. Department of Energy by Lawrence Livermore National Laboratory under Contract DE-AC52-07NA27344. Funding was provided by the DOE Office of Energy Efficiency and Renewable Energy, and the Lawrence Livermore National Laboratory Directed Research and Development (LDRD) Grant 12-ERD-035 and 13-LW-099.

Notes and references

Electronic Supplementary Information (ESI) available: Experimental methods, supplementary figures and discussion. See DOI: 10.1039/c000000x/

1. M. A. Worsley, S. O. Kucheyev, H. E. Mason, M. D. Merrill, B. P. Mayer, J. Lewicki, C. A. Valdez, M. E. Suss, M. Stadermann, P. J. Pauzauskie, J. H. Satcher, J. Biener and T. F. Baumann, Chemical Communications **48** (67), 8428-8430 (2012).
2. T. F. Baumann, M. A. Worsley, T. Y.-J. Han and J. H. Satcher Jr, Journal of Non-Crystalline Solids **354** (29), 3513-3515 (2008).
3. C. Vix-Guterl, E. Frackowiak, K. Jurewicz, M. Friebe, J. Parmentier and F. Béguin, Carbon **43** (6), 1293-1302 (2005).
4. Y. Zhu, H. Hu, W. Li and X. Zhang, Carbon **45** (1), 160-165 (2007).
5. C. Emmenegger, P. Mauron, P. Sudan, P. Wenger, V. Hermann, R. Gallay and A. Züttel, Journal of Power Sources **124** (1), 321-329 (2003).
6. L. Basirico and G. Lanzara, Nanotechnology **23** (30), 305401 (2012).
7. C. Niu, E. K. Sichel, R. Hoch, D. Moy and H. Tennent, Applied Physics Letters **70** (11), 1480-1482 (1997).
8. C. Du, J. Yeh and N. Pan, Nanotechnology **16** (4), 350 (2005).
9. A. Lewandowski and M. Galinski, Journal of Power Sources **173** (2), 822-828 (2007).
10. L. L. Zhang and X. Zhao, Chemical Society Reviews **38** (9), 2520-2531 (2009).
11. R. Kötz and M. Carlen, Electrochimica Acta **45** (15), 2483-2498 (2000).
12. X. Yang, C. Cheng, Y. Wang, L. Qiu and D. Li, Science **341** (6145), 534-537 (2013).
13. Y. Tao, X. Xie, W. Lv, D.-M. Tang, D. Kong, Z. Huang, H. Nishihara, T. Ishii, B. Li and D. Golberg, Scientific reports **3** (2013).
14. J. Hu, Z. Kang, F. Li and X. Huang, Carbon **67**, 221-229 (2014).
15. M. F. El-Kady, V. Strong, S. Dubin and R. B. Kaner, Science **335** (6074), 1326-1330 (2012).
16. T. Kim, G. Jung, S. Yoo, K. S. Suh and R. S. Ruoff, ACS nano **7** (8), 6899-6905 (2013).
17. Y. J. Kim, C. M. Yang, K. C. Park, K. Kaneko, Y. A. Kim, M. Noguchi, T. Fujino, S. Oyama and M. Endo, ChemSusChem **5** (3), 535-541 (2012).
18. F. B. Sillars, S. I. Fletcher, M. Mirzaeian and P. J. Hall, Energy & Environmental Science **4** (3), 695-706 (2011).
19. R. K. Kalluri, M. M. Biener, M. E. Suss, M. D. Merrill, M. Stadermann, J. G. Santiago, T. F. Baumann, J. Biener and A. Striolo, Physical Chemistry Chemical Physics **15** (7), 2309-2320 (2013).
20. C. Largeot, C. Portet, J. Chmiola, P.-L. Taberna, Y. Gogotsi and P. Simon, Journal of the American Chemical Society **130** (9), 2730-2731 (2008).
21. R. Gilliam, J. Graydon, D. Kirk and S. Thorpe, International Journal of Hydrogen Energy **32** (3), 359-364 (2007).
22. K. Fic, G. Lota, M. Meller and E. Frackowiak, Energy & Environmental Science **5** (2), 5842-5850 (2012).
23. Q. Gao, L. Demarconnay, E. Raymundo-Piñero and F. Béguin, Energy & Environmental Science **5** (11), 9611-9617 (2012).
24. K. Fic, E. Frackowiak and F. Béguin, Journal of Materials Chemistry **22** (46), 24213-24223 (2012).
25. W. M. Haynes, *CRC handbook of chemistry and physics*. (CRC press, 2012).

TOC Entry

High-density electrodes allow aqueous-based supercapacitors to attain energy densities comparable to those of commercially-available organic-based supercapacitors with 10 - 100× greater power.